

GL00367

FC
USGS
OFR
80-688

UNITED STATES
DEPARTMENT OF THE INTERIOR
GEOLOGICAL SURVEY

SCINTILLATION DETECTORS IN GAMMA SPECTRAL LOGGING:
GEOMETRY, ABSORPTION AND CALIBRATION
BY Ulrich Schimschal

U.S. Geological Survey

WATER RESOURCES INVESTIGATIONS

OPEN FILE REPORT 80-688

UNIVERSITY OF UTAH
RESEARCH INSTITUTE
EARTH SCIENCE LAB.

Denver, Colorado
1980

For additional copies write to:

U.S. Geological Survey
Open-File Services Section
Branch of Distribution
Box 25425, Federal Center
Denver, Colorado 80225

Table of Contents

	page
Abstract-----	1
Introduction-----	2
Theory-----	3
Attenuation through absorbing media-----	3
Geometrical spreading-----	4
Total intensity from a point source gamma emitter incident on the cylindrical surface of a cylindrical detector-----	5
Total intensity from a point source gamma emitter absorbed by a cylindrical detector neglecting end-on radiation-----	11
Theoretical Results-----	21
Evaluation of Experimental Data-----	23
Conclusions-----	28
References-----	29

List of Illustrations

	page
Figure 1 -- Radiation incident on the cylindrical surface of a detector crystal-----	7
Figure 2 -- Plan view of cylindrical detector-----	8
Figure 3 -- Limits of integration-----	10
Figure 4 -- Radiation intensity at a given point inside the detector due to a point source located outside the detector-----	12
Figure 5 -- Theoretical curves constructed from model considering only radiation incident and emerging from the cylindrical surface of the crystal. The source intensity is equal to unity. The source-detector distance is to the surface of the detector-----	22
Figure 6 -- Mathematical model used in constructing theoretical curves; radiation through the ends of the crystal has been neglected in this model-----	24
Figure 7 -- Comparison of experimental points to theoretical curves. The experimental curves have been corrected for the instrumentation coefficient-----	25
Figure 8 -- Calibration of NaI cylindrical detectors using "point" sources. The instrumentation coefficient is obtained experimentally and accounts for efficiency in conversion of incident gamma energy to electrical energy output from PM tube-----	27

SCINTILLATION DETECTORS IN GAMMA SPECTRAL LOGGING:
GEOMETRY, ABSORPTION AND CALIBRATION

By

Ulrich Schimschal

Abstract

The theory for the evaluation of the effects of geometry in gamma ray absorption is developed for cylindrical scintillation detectors as applicable to borehole gamma spectrometry. The results of a laboratory experiment are shown for comparison. A calibration procedure to determine detector efficiency is given for application to borehole probes. It is shown that the response of a crystal can be separated in terms of geometric effects and instrumentation effects. It is also shown that approximating crystal detectors with point detectors in mathematical theory is grossly oversimplified.

Introduction

The theoretical response of spectral gamma-ray logging probes for various borehole conditions is usually calculated by assuming that the probe is a point or line detector in the borehole. However, sizable response differences between theoretical calculations and field data can be attributed to the fact that the geometry and absorption characteristics of the scintillation crystal of the probe is not a point or a line source. The effects caused by the geometry and absorption of the crystal can be calculated from mathematical models and verified by experiment. The total efficiency with which the combination of crystal and photomultiplier tube convert incident gamma energy into detectable counts in the multichannel analyzer can be determined experimentally, after correcting the data for the effects of geometry and absorption in the crystal. The efficiency of energy conversion can be corrected by multiplying the response by a coefficient. This approach then is designed to separate the effects on the gamma-ray spectrum from those effects that fall into the realm of visible light and the subsequent conversion of the light into electrical impulses. Once the effect of the crystal and a point source is calculated, the effect of distributed sources, made up from volume elements representative of point sources, can be calculated by numerical integration. In order to quantify spectral data obtained in the borehole, these detector effects have to be incorporated into the interpretive process in the analysis of field data.

Theory

Attenuation through absorbing media

Experimental data for the absorption of gamma rays passing through a medium can be approximated by the following mathematical expression:

$$I = I_0 e^{-\mu R} \quad (1)$$

where I = intensity or count rate after passage through thickness R of absorber material

I_0 = intensity or count rate from a given source when no absorber is used

μ = linear attenuation coefficient, units reciprocal to (R) units

R = distance through which radiation is absorbed

The above relationship holds for conditions where the gamma beam is homogenous and collimated, and the absorber material is thin.

Geometrical Spreading

Loss in intensity due to geometrical spreading is a common occurrence with physical phenomena. When considering a small volume of radiating material (essentially a point source) one should expect that over a period of time radiation will escape uniformly in all directions. Intensity measured some distance away from the point source will then be diminished as a function of distance (fig. 1).

$$I = \frac{I_0 e^{-\mu R}}{4\pi R^2} \quad (2)$$

where I is the intensity at a distance R away from a small source with specific activity I_0 , and μ is the linear attenuation coefficient.

Total intensity from a point source gamma emitter incident on the cylindrical surface of a cylindrical detector

In order to increase the accuracy of the model and hence approach more closely the conditions encountered in the hole, the effect of a cylindrical detector will be treated next (fig. 1). In the discussion that follows only the total gamma radiation from a small source volume incident on the cylindrical surface of a right circular cylinder will be considered. Loss from this cylinder adds an additional degree of complexity and will be discussed as a separate topic.

Let us consider radiation flux ϕ of intensity I penetrating the surface of a cylindrical detector crystal at an arbitrary angle δ .

Then
$$\phi = \int_S \bar{I} \cdot \bar{\Delta S}$$

or
$$\phi = \int_S I \cos \delta \Delta S \tag{3}$$

where \bar{I} = vector intensity

$\bar{\Delta S}$ = surface vector

ϕ = radiation flux

Using cylindrical coordinates, we get

$$\Delta S = \Delta z r \Delta \theta = \Delta z \frac{d}{2} \Delta \theta \tag{4}$$

Let the source be located at $P_0 (r_0, \theta_0, z_0)$, and let the surface element ΔS be located at $P (\frac{d}{2}, \theta, z)$. The total magnitude of the radiation incident upon the cylindrical surface can then be found by integrating over the appropriate boundary. The following expressions are useful in obtaining a tractable expression:

$$\frac{z_0 - z}{R} = \sin \phi \quad (5)$$

$$\frac{x}{R} = \cos \delta \quad (6)$$

$$R^2 = y^2 + (z_0 - z)^2 \quad (7)$$

$$\frac{x + \frac{d}{2}}{r_0} = \cos \theta; \quad x = r_0 \cos \theta - \frac{d}{2} \quad (8)$$

$$y^2 = \left(\frac{d}{2}\right)^2 + r_0^2 - 2 \frac{d}{2} r_0 \cos \theta \quad (9)$$

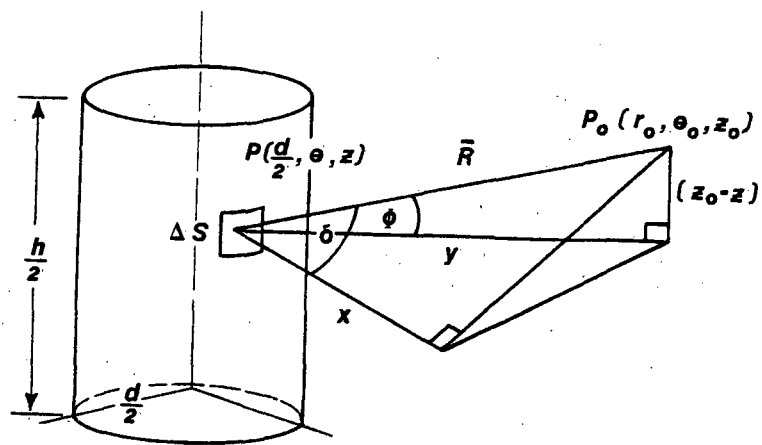


Figure 1.--Radiation incident on the cylindrical surface of a detector crystal

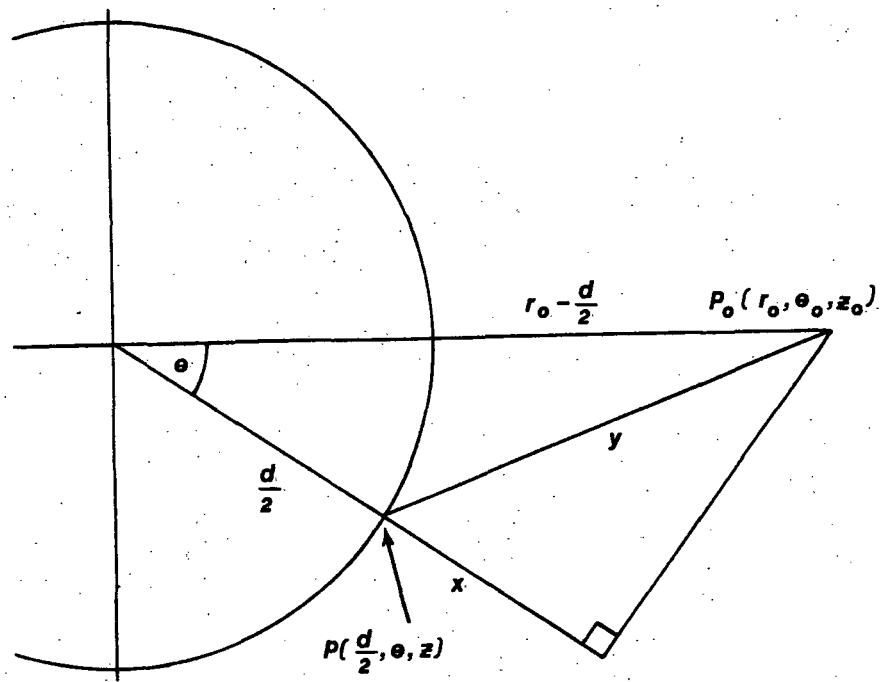


Figure 2.--Plan view of cylindrical detector

Combining equations (5) through (9) we obtain the following expression:

$$\cos \delta = \frac{r_o \cos \theta - \frac{d}{2}}{R} \quad (10)$$

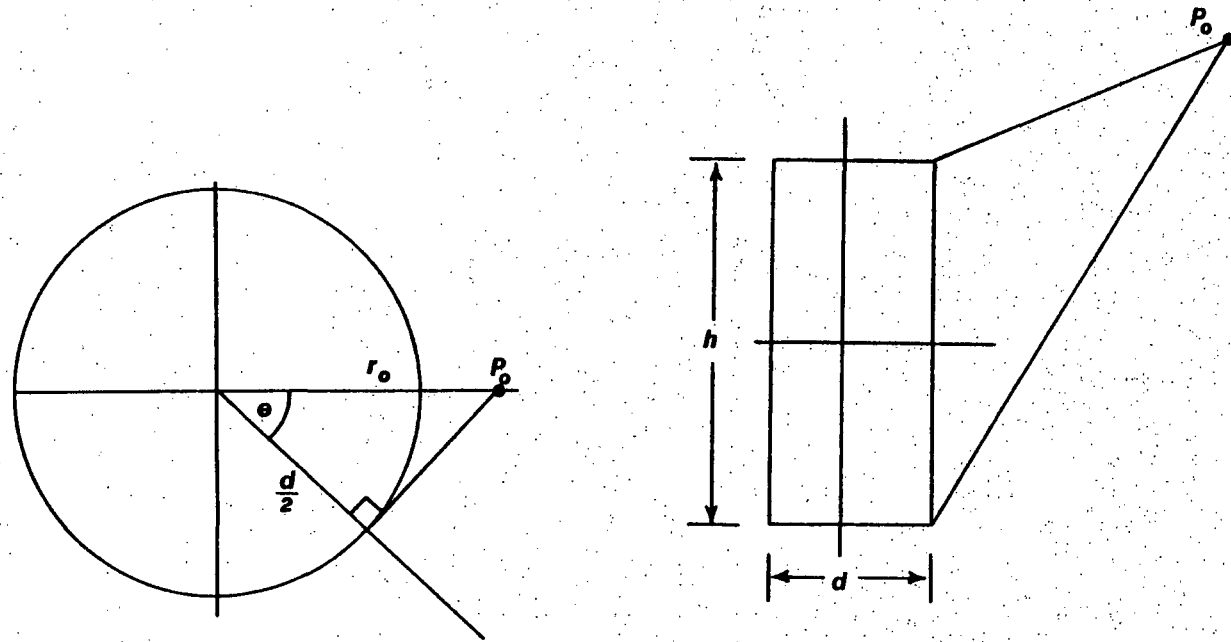
$$R^2 = \left(\frac{d}{2}\right)^2 + r_o^2 - dr_o \cos \theta + (z_o - z)^2 \quad (11)$$

From (3) and (2), using (8), (9), and (4) we obtain the following integrable equation:

$$\Phi = I_o \int_{\theta_1}^{\theta_2} \int_{z_1}^{z_2} \frac{\exp \left(-\mu \left[\left(\frac{d}{2}\right)^2 + r_o^2 - dr_o \cos \theta + (z_o - z)^2 \right]^{1/2} \right)}{4\pi \left[\left(\frac{d}{2}\right)^2 + r_o^2 - dr_o \cos \theta + (z_o - z)^2 \right]^{3/2}} \left(r_o \cos \theta - \frac{d}{2} \right) \frac{d}{2} dzd\theta \quad (12)$$

The limits of integration are shown in Figure 3. There it can be seen that depending on the location of the source only a portion of the cylinder will be intercepted by incoming radiation. Both the top and bottom of the cylindrical crystal are assumed to be shielded.

Equation (12) is not solvable in closed form, and is therefore solved numerically on a computer.



$$\theta_1 = 0$$

$$\theta_2 = \cos^{-1} \frac{d}{2r_0}$$

$$z_1 = -\frac{h}{2}$$

$$z_2 = \frac{h}{2}$$

Figure 3.—Limits of integration

Total Intensity from a Point Source Gamma Emitter
Absorbed by a Cylindrical Detector Neglecting end-on Radiation

As mentioned earlier not all of the radiation incident upon a detector is absorbed. In calculating total intensity only the absorbed portion of the radiation will result in a measurable response in the photomultiplier tube. For the discussion that follows the reader is referred to figure 4.

If $I(P)$ represents the intensity at a volume element $dV(r, \theta, z)$ inside the detector and R is the total distance between source and volume element within the detector and R_s is that portion of the total distance outside the detector and R_d is that portion of the total distance inside the detector; then

$$I(P) = \frac{I_0 e^{-(\mu_s R_s + \mu_d R_d)}}{4\pi (R_s + R_d)^2} \quad (13)$$

where μ_s, μ_d are the attenuation coefficients of the source and detector materials, respectively.

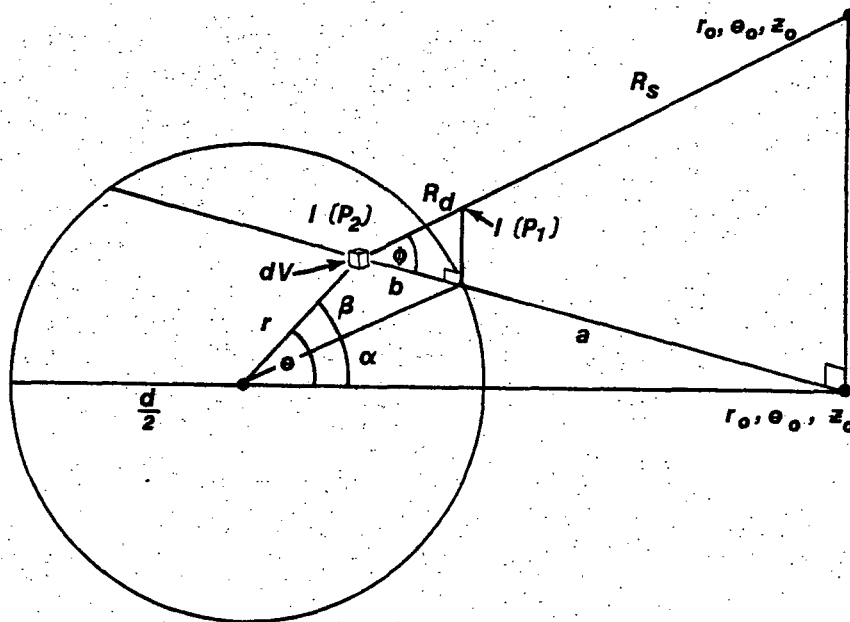


Figure 4.--Radiation intensity at a given point inside the detector due to a point source located outside the detector

From figure 4 let R' be the projection of R onto an arbitrary plane perpendicular to the z -axis, then

$$R = R_s + R_d \quad (14)$$

$$R' = a + b \quad (15)$$

$$a^2 = \left(\frac{d}{2}\right)^2 + r_o^2 - dr_o \cos \alpha \quad (16)$$

$$b^2 = \left(\frac{d}{2}\right)^2 + r^2 - dr \cos \beta \quad (17)$$

$$\alpha + \beta = \theta \quad (18)$$

$$R'^2 = r^2 + r_o^2 - 2rr_o \cos \theta \quad (19)$$

$$\frac{b}{R_d} = \cos \phi \quad (20)$$

$$\phi = \tan^{-1} \frac{z_o - z}{R'} \quad (21)$$

$$R^2 = R'^2 + (z_o - z)^2 \quad (22)$$

Combining and simplifying equations (15, 16, 17, and 18) we obtain:

$$a^2 = \left(\frac{d}{2}\right)^2 + r_o^2 - 2 \left(\frac{d}{2}\right) r_o \cos (\theta - \beta) \quad (23)$$

where $\beta = \cos^{-1} \frac{r_o^2 + \left(\frac{d}{2}\right)^2 - (R' - a)^2}{dr}$ (24)

From (23) we obtain the following equations:

$$\cos \theta \cos \beta + \sin \theta \sin \beta = \frac{\left(\frac{d}{2}\right)^2 + r_o^2 - a^2}{d r_o}$$

$$\sin \beta = \frac{\left(\frac{d}{2}\right)^2 + r_o^2 - a^2}{\sin \theta d r_o} - \frac{\cos \theta \cos \beta}{\sin \theta} \quad (25)$$

Using the trigonometric identity $\sin^2 \beta = 1 - \cos^2 \beta$, equation (26) can be written as:

$$1 - \cos^2 \beta = \left[\frac{\left(\frac{d}{2}\right)^2 + r_o^2 - a^2}{\sin \theta d r_o} - \frac{\cos \theta}{\sin \theta} \cos \beta \right]^2 \quad (26)$$

Equation (26) can be rewritten as follows, in order to solve for "a":

$$1 - \cos^2 \beta = \frac{\left(\left(\frac{d}{2}\right)^2 + r_0^2 - a^2\right)^2}{\sin^2 \theta d^2 r_0^2} + \frac{\cos^2 \theta}{\sin^2 \theta} \cos^2 \beta$$

$$- 2 \frac{\left(\left(\frac{d}{2}\right)^2 + r_0^2 - a^2\right) \cos \theta \cos \beta}{\sin^2 \theta d r_0}$$

$$1 - \frac{\cos^2 \beta}{\sin^2 \theta} = \frac{\left(\left(\frac{d}{2}\right)^2 + r_0^2 - a^2\right)^2}{\sin^2 \theta d^2 r_0^2}$$

$$- 2 \frac{\left(\left(\frac{d}{2}\right)^2 + r_0^2 - a^2\right) \cos \theta \cos \beta}{\sin^2 \theta d r_0}$$

$$\sin^2 \theta - \frac{\left[r^2 + \left(\frac{d}{2}\right)^2 - (R' - a)^2\right]^2}{d^2 r^2} = \frac{\left(\left(\frac{d}{2}\right)^2 + r_0^2 - a^2\right)^2}{d^2 r_0^2}$$

$$- \frac{2 \cos \theta}{d^2 r_0 r} \left(\left(\frac{d}{2}\right)^2 + r_0^2 - a^2\right) \left(r^2 + \left(\frac{d}{2}\right)^2 - (R' - a)^2\right)$$

(27)

$$d^2 r^2 r_0^2 \sin^2 \theta - [r_0^2] \left[r^2 + \left(\frac{d}{2}\right)^2 - (R' - a)^2 \right]^2 - r^2 \left(\left(\frac{d}{2}\right)^2 + r_0^2 - a^2 \right)^2$$

$$+ 2 r r_0 \cos \theta \left(\left(\frac{d}{2}\right)^2 + r_0^2 - a^2 \right) \left(r^2 + \left(\frac{d}{2}\right)^2 - (R' - a)^2 \right) = 0$$

To simplify notation, let $c = r^2 + \left(\frac{d}{2}\right)^2$, and $c_0 = r_0^2 + \left(\frac{d}{2}\right)^2$, then

$$d^2 r^2 r_0^2 \sin^2 \theta - r_0^2 \left[c - R'^2 - a^2 + 2 a R' \right]^2 - r^2 (c_0 - a^2)^2$$

$$+ 2 r r_0 \cos \theta (c_0 - a^2) (c - R'^2 - a^2 + 2 a R') = 0$$

$$d^2 r^2 r_0^2 \sin^2 \theta - r_0^2 \left[c^2 - c R'^2 - c a^2 + 2 a R' c - c R'^2 + R'^4 + R'^2 a^2 \right.$$

$$\left. - 2 a R'^3 - c a^2 + a^2 R'^2 + a^4 - 2 a^3 R' + 2 a R' c - 2 a R'^3 - 2 a^3 R' \right.$$

$$\left. + 4 a^2 R'^2 \right] - r^2 \left[c_0^2 + a^4 - 2 c_0 a^2 \right] + 2 r r_0 \cos \theta \left[c_0 c \right.$$

$$\left. - c_0 R'^2 - c_0 a^2 + 2 a R' c_0 - c a^2 + a^2 R'^2 + a^4 - 2 a^3 R' \right] = 0$$

Collecting terms in powers of a, we get:

$$a^4 \left[-r_0^2 - r^2 + 2 r r_0 \cos \theta \right] +$$

$$a^3 \left[+ 4 R' r_0^2 - 4 r r_0 R' \cos \theta \right] +$$

$$a^2 \left[2r_0^2 c - 6 r_0^2 R'^2 + 2 r^2 c_0 + 2 r r_0 \cos \theta (-c_0 - c + R'^2) \right] +$$

$$a \left[-r_0^2 4R'c + r_0^2 4R'^3 + 2 r r_0 \cos \theta 2R'c_0 \right]$$

$$+ \left[d^2 r^2 r_0^2 \sin^2 \theta - r_0^2 (c^2 - 2cR'^2 + R'^4) - r^2 c_0^2 + 2 r r_0 \cos \theta \right.$$

$$\left. (c_0 c - c_0 R'^2) \right] = 0$$

(28)

Equation (28) is a quartic equation in "a" and can be solved in terms of its coefficients (see Handbook of Tables for Mathematics, 1962, 4th ed., The Chemical Rubber Co., p. 132).

$$\begin{aligned}
 \text{let } A(r, z, \theta) &= -r_0^2 - r^2 + 2rr_0 \cos \theta \\
 B(r, z, \theta) &= 4R'r_0^2 - 4rr_0R' \cos \theta \\
 C(r, z, \theta) &= 2r_0^2c - 6r_0^2R'^2 + 2r^2c_0 \\
 &\quad + 2rr_0 \cos \theta (-c_0 - c + R'^2) \\
 D(r, z, \theta) &= -r_0^24R'c + r_0^24R'^3 + 4rr_0 \cos \theta R'c_0 \\
 E(r, z, \theta) &= d^2r^2r_0^2 \sin^2 \theta - r_0^2 (c^2 - 2cR'^2 + R'^4) \\
 &\quad - r^2c_0^2 + 2rr_0 \cos \theta (c_0c - c_0R'^2)
 \end{aligned} \tag{29}$$

then, from (29) and (30)

$$a^4 + \frac{B}{A} a^3 + \frac{C}{A} a^2 + \frac{D}{A} a + \frac{E}{A} = 0$$

$$\text{let } \frac{B}{A} = c_1; \frac{C}{A} = c_2; \frac{D}{A} = c_3; \frac{E}{A} = c_4$$

$$\text{then } a = -\frac{c_1}{4} + \frac{K}{2} \pm \frac{F}{2}$$

$$\text{and } a = -\frac{c_1}{4} - \frac{K}{2} \pm \frac{N}{2} \tag{30}$$

where the resolvent cubic equation is

$$y^3 - c_2y^2 + (c_1c_3 - 4c_4)y - c_1^2c_4 + 4c_2c_4 - c_3^2 = 0 \tag{31}$$

$$K = \sqrt{\frac{c_1^2}{4} - c_2 + y} \quad \text{where } y \text{ is any root of the above equation}$$

if $K \neq 0$, then let

$$F = \left[\frac{3c_1^2}{4} - K^2 - 2c_2 + \frac{4c_1c_2 - 8c_3 - c_1^3}{4K} \right]^{1/2}$$

$$\text{and } N = \left[\frac{3c_1^2}{4} - K^2 - 2c_2 + \frac{4c_1c_2 - 8c_3 - c_1^3}{4K} \right]^{1/2}$$

If $K = 0$, then let

$$F = \left[\frac{3c_1^2}{4} - 2c_2 + 2(y^2 - 4c_4)^{1/2} \right]^{1/2}$$

and

$$N = \left[\frac{3c_1^2}{4} - 2c_2 - 2(y^2 - 4c_4)^{1/2} \right]^{1/2}$$

Equation (31) can be solved also in terms of its coefficients. Details are given in the Handbook of Tables of Mathematics, p. 129.

After solving for "a" from (30) we can express (with the use of equations (14) through (22)) both R_s and R_d as function of r, θ, z . Equation (13) can be solved numerically on the computer. The total radiation leaving the surface of the crystal after absorption through the crystal can be expressed as:

$$I_p(r_o, \theta_o, z_o) = \int \frac{I_o e^{-\mu_s R_s(r, \theta, z)} e^{-\mu_d R_d(r, \theta, z)}}{4\pi R^2(r, \theta, z)} \frac{\overline{n} \cdot \overline{\Delta S}}{\Delta S} \quad (32)$$

where $I_p(r_o, \theta_o, z_o)$, is the total intensity detected due to a point source located at (r_o, θ_o, z_o) , where $\overline{\Delta S}$ is the surface vector and \overline{n} is the unit vector in the direction of the gamma ray.

THEORETICAL RESULTS

The results of the theoretical discussion presented above were programmed for computer evaluation. The program, written in Fortran, was evaluated for a point source located in the midplane of a cylindrical detector crystal. The crystal was assumed to be NaI (sodium iodide) with a density of $\rho = 3.667$. The point source was assumed to be Cs¹³⁷ with an energy peak at 661 Kev and unit source intensity. The surrounding medium was considered to be air. Linear attenuation coefficients, interpolated for 661 Kev from the Radiological Health Handbook were for air $\mu_L = 9.3 \cdot 10^{-5}/\text{cm}$, and for NaI $\mu_L = 0.29/\text{cm}$. Total intensity absorbed by the detector crystal was calculated for source-detector spacings ranging from 2 to 34 inches. These calculations were made for the three crystal sizes presently in use at the U. S. Geological Survey, Water Resources Division, Borehole Geophysics Research Project. The crystal sizes are given in terms of diameter x length in inches; 1 1/4 x 4, 3 x 3, and 3 x 12. For each crystal size, the following theoretical results were plotted as a function of distance from the edge of the crystal:

- a. incident radiation onto the cylindrical face of the crystal, and
- b. total absorbed radiation in the crystal

The total absorbed intensity for a unit source at a given energy level has been called K_d - detector coefficient.

The results of this evaluation have been plotted in Figure 5. For comparison the results for a point detector have also been plotted on the same graph.

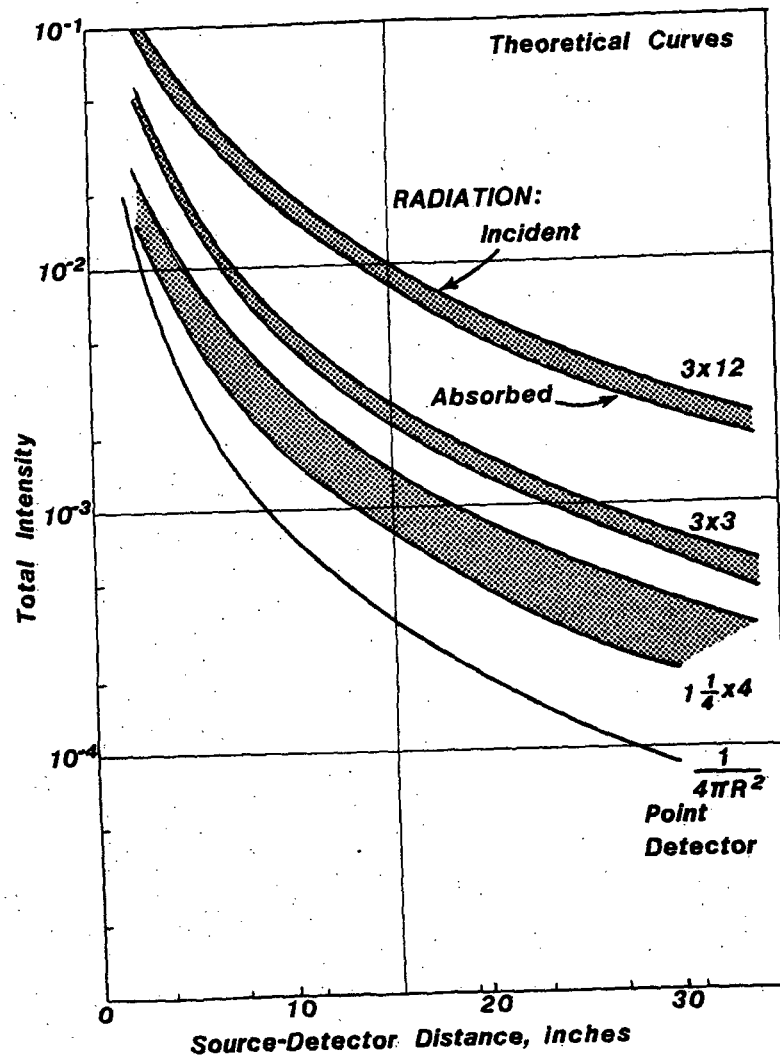


Figure 5.--Theoretical curves constructed from model considering only radiation incident and emerging from the cylindrical surface of the crystal. The source intensity is equal to unity. The source-detector distance is to the surface of the detector.

Evaluation of Experimental Data

The accuracy of the theory was tested experimentally. The experimental setup is shown in Figure 6. The source was Cs¹³⁷, peak energy at 661 Kev, source intensity $I_0 = 1.4 \mu\text{Ci} \pm 0.1$. The source, enclosed in a plastic disk, was moved in the midplane of the cylindrical NaI detector and placed on its edge. A background spectrum was obtained before and after the experiment for a duration of 1000 seconds. The test itself was also conducted over a period of 1000 seconds. Background was then subtracted. Figure 7 shows the experimental data. Only the number of counts within the photopeak area were plotted. The results have been corrected for K_I , a calibration coefficient accounting for conversion efficiency between crystal and photomultiplier tube. The calculation of the instrumentation coefficient K_I is given as:

Source Cs¹³⁷, peak at 661 Kev

Source strength, $I_0 = 1.4 \mu\text{Ci}$

Gamma abundance at 661 Kev, $\gamma = 84.62$ percent

Total intensity at peak channel, $I_t = 231$ cps

or $231 \div 37,000 = 6.24 \cdot 10^{-3} \mu\text{Ci}$

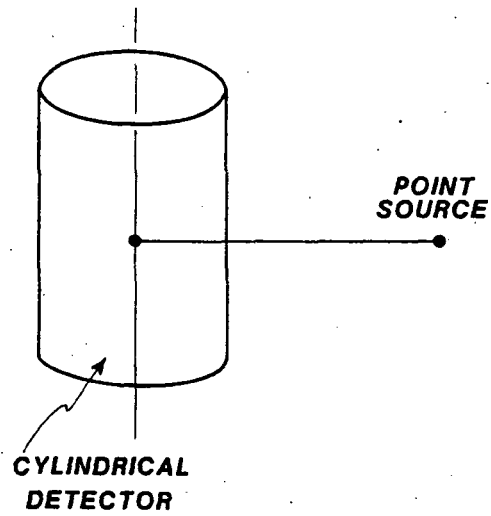


Figure 6.--Mathematical model used in constructing theoretical curves; radiation through the ends of the crystal has been neglected in this model.

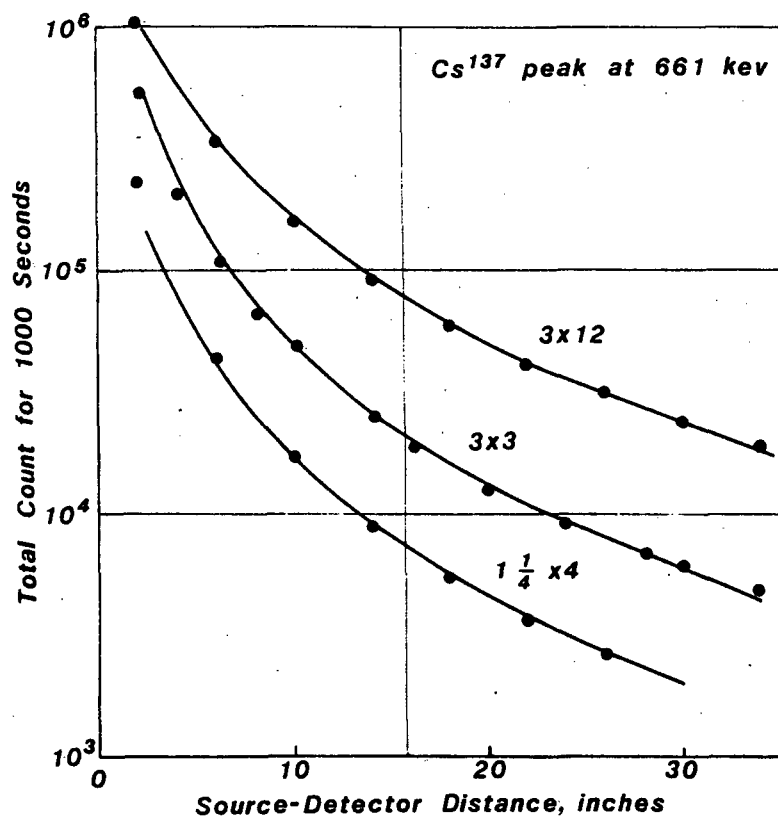


Figure 7.--Comparison of experimental points to theoretical curves. The experimental curves have been corrected for the instrumentation coefficient.

From theory the detector coefficient, K_d , calculated for a distance of 6 inches from the crystal is for the 3 x 3 crystal, $K_d = 0.0125$ we then have:

$$I_t = I_0 \gamma K_d K_I$$

$$\text{or } K_I = \frac{I_t}{I_0 \gamma K_d} = \frac{6 \cdot 24 \cdot 10^{-3}}{1.4 \cdot 0.8462 \cdot 0.0125} = 0.4216$$

The curves in Figure 7 show that this correction for K_I gives a close fit to the experimental data. Figure 8 shows the results of calibrations to determine the instrumentation coefficient, K_I , as a function of energy for various crystal sizes.

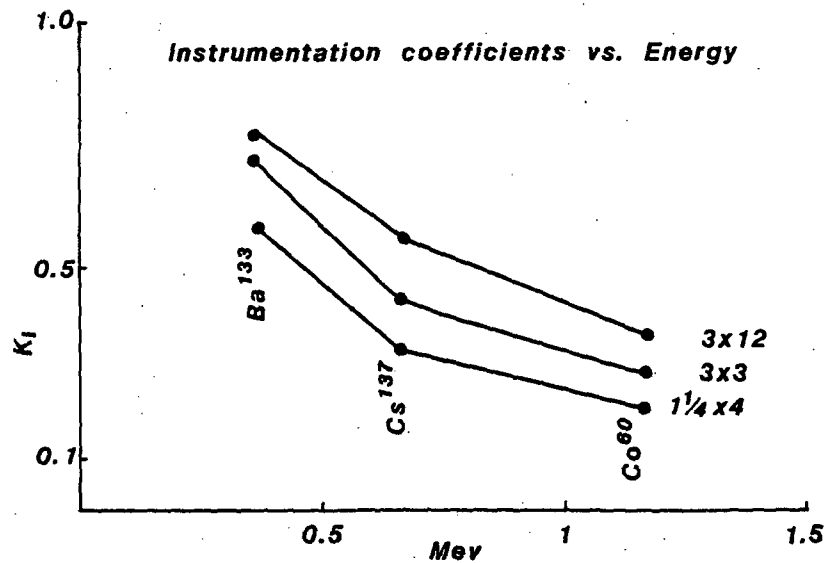


Figure 8.--Calibration of NaI cylindrical detectors using "point" sources. The instrumentation coefficient is obtained experimentally and accounts for efficiency in conversion of incident gamma energy to electrical energy output from PM tube.

Conclusions

The results of this study can be summarized as follows:

1. The effect of assuming a finite volume detector can be calculated with reasonable accuracy.
2. The calibration of detector effects for the quantitative borehole evaluation of gamma spectra recorded in a borehole can then be accomplished in the same manner as in this experiment.
3. The assumption of point detectors in the calculation of borehole effects or bed thickness can cause sizable errors, because the scintillation crystal has geometric and absorption characteristics that are dissimilar to a point source. Calibration to account for non-point source probe effects is required.

References

- Adams, John S., and Gasparini, Paolo, 1970, Gamma-ray spectrometry of rocks: Elsevier Publishing Company, 256 p.
- Barsukov, O. A., Blinova, N. M., Vybornykh, S. F., Gulin, Yu. A., Dakhnov, V. N., Larionov, V. V., and Kholin, A. I., 1965, Radioactive investigations of oil and gas wells: Pergamon Press, 289 p.
- Bureau of Radiological Health and Training Institute Environmental Control Administration, 1970, Radiological health handbook: U.S. Department of Health, Education, and Welfare, Public Health Service, January, 458 p.
- Goldstein, Herbert, and Wilkins, Ernest J., Jr., 1954, Calculations of the penetration of gamma-rays: Atomic Energy Commission, June, 196 p.
- Heath, R. L., 1964, Scintillation spectrometry, gamma-ray spectrum catalogue: I. D. O. Report 16880-1, second ed., August, v. 1, 264 p., v. 2, 239 p.
- Heath, R. L., Helmer, R. G., Schmittroth, L. A., and Cazier, G. A., 1965, The calculation of gamma-ray shapes for sodium iodide scintillation spectrometers: I. D. O. Report 17017, April, 158 p.
- Lederer, C. M., Hollander, J. M., and Perlman, I., 1967, Table of isotopes: John Wiley and Sons, 594 p.
- Mathews, M. A., Koizumi, C. J., Evans, Hilton, B. E., 1978, DOE-Grand Junction logging model data synopsis: Bendix Field Engineering Corporation, May, GJBX-76(78), 52 p.
- Quittner, P., 1972, Gamma-ray spectroscopy with particular reference to detector and computer evaluation techniques: Adam Hilger Ltd., London, 111 p.
- Radiological Health Branch Training Institute, 1967, Radionuclide analysis by gamma spectroscopy: U.S. Department of Health, Education, and Welfare, Public Health Service, Consumer Protection Environmental Health Service, August.